

Adsorption of CO on ordered alloy surfaces

S. H. Lu

Department of Physics, Peking University, Beijing 100871, China

J. Yao

Synchrotron Radiation Laboratory, Institute of High Energy Physics, Academia Sinica, Beijing 100039, China

L. Zhu

Department of Physics, Zhejiang University, Hangzhou 310027, China

G. L. Liu

Department of Physics, Yantai University, Yantai 264005, China

F. Q. Liu

Synchrotron Radiation Laboratory, Institute of High Energy Physics, Academia Sinica, Beijing 100039, China

S. C. Wu

*Department of Physics, Peking University, Beijing 100871, China
and Laboratory for Surface Physics, Academia Sinica, Beijing 100080, China*

(Received 21 May 1991)

The adsorption of CO on two ordered alloy surfaces, $\text{Cu}\{001\}c(2\times 2)\text{-Pd}$ and $\text{Ni}\{001\}c(2\times 2)\text{-Al}$, has been studied by high-resolution electron-energy-loss spectroscopy. For $\text{Cu}\{001\}c(2\times 2)\text{-Pd}$, CO molecules are bonded only in on-top positions of Pd atoms at 240 K; at 135 K, CO molecules are bonded in on-top positions of Pd atoms also for low coverage, and CO adsorbed both in on-top positions of Pd and Cu atoms for high coverage. For oxygen-contaminated $\text{Ni}\{001\}c(2\times 2)\text{-Al}$, CO molecules are bonded in on-top positions of Ni atoms and fourfold bridge positions between two Ni and two Al atoms, and the dissociation of CO has been observed at room temperature and low temperatures. The CO-dissociation rate is proportional to the degree of oxygen contamination on the surface.

I. INTRODUCTION

Ordered alloy surfaces, which are known to have a stable, well-defined structure, provide the possibility of relating surface properties with microscopic data. An example is $\text{Cu}\{001\}c(2\times 2)\text{-Pd}$,¹ which is usually obtained from depositing a half monolayer of Pd onto a clean $\text{Cu}\{001\}$ surface. In our earlier work,¹ low-energy electron diffraction (LEED) intensity analysis showed that the top layer is an ordered 50%-50% mixture of Pd and Cu atoms and almost coplanar, with the Pd atoms located 0.02 ± 0.03 Å outward from the Cu atoms. The second layer is 100% Cu. The $\text{Cu}\{001\}c(2\times 2)\text{-Pd}$ surface is the equivalent surface of a Cu_3Pd bulk alloy. Another example is $\text{Ni}\{001\}c(2\times 2)\text{-Al}$,² which was obtained from depositing approximately 0.75 monolayer Al onto $\text{Ni}\{001\}$ heated at 250°C or depositing Al onto an unheated Ni substrate and annealing at 550°C for five min. The LEED spectra of $\text{Ni}\{001\}c(2\times 2)\text{-Al}$ are very similar to those of $\text{Ni}_3\text{Al}\{001\}$.

Graham³ has studied the chemisorption of CO on a $\text{Cu}\{001\}c(2\times 2)\text{-Pd}$ by ultraviolet photoelectron spectroscopy (UPS) and found that the chemisorption of CO on $\text{Cu}\{001\}c(2\times 2)\text{-Pd}$ surface occurs molecularly with a saturation coverage at 100 K, which is approximately the

same as that on $\text{Cu}\{001\}$. Franchy⁴ have studied the adsorption of CO on the ordered alloy $\text{NiAl}\{111\}$. At 300 K, CO is adsorbed in an on-top position. At 80 K and full CO coverage the CO molecules are adsorbed at on-top positions with an admixture of tilted bridge positions between first-layer Ni atoms and second-layer Al atoms.

In this paper we report on the adsorption of CO on $\text{Cu}\{001\}c(2\times 2)\text{-Pd}$ and on $\text{Ni}\{001\}c(2\times 2)\text{-Al}$ studied by LEED, Auger electron spectroscopy (AES) and high-resolution electron-energy-loss spectroscopy (HREELS). For $\text{Cu}\{001\}c(2\times 2)\text{-Pd}$, CO molecules are bonded only in on-top positions of Pd atoms at 240 K; at 135 K, CO molecules are bonded in on-top positions of Pd atoms at low coverage and CO is adsorbed in on-top position of both Pd and Cu atoms at high coverage. For oxygen-contaminated $\text{Ni}\{001\}c(2\times 2)\text{-Al}$, CO molecules are bonded in on-top positions of Ni atoms and fourfold bridge positions between two Ni and two Al atoms and the dissociation of CO has been observed at room temperature and low temperature. The CO-dissociation rate is proportional to the degree of oxygen contamination on the surface.

II. EXPERIMENTS

The experiments were carried out in a stainless-steel ultrahigh vacuum system (Leybold-Heraeus) equipped with

a four-grid optics for LEED and AES and a double-pass high-resolution electron-energy-loss spectrometer. All HREELS data were collected in the specular direction with a total scattering angle of 120° and an incident beam energy of 5.0 eV. Typical resolution (full width at half maximum) was in the range 10–14 meV in the elastic peak.

The Cu{001} single crystal was cleaned *in situ* by repeated cycles of Ar-ion sputtering and heating until the S, C, and O Auger signals disappeared within the limits of the noise level of the Auger spectra. A well-ordered 1×1 surface was confirmed by LEED at this stage. The sample-mounting stage provided for liquid-nitrogen cooling to 135 K and electron bombardment and/or radiation heating to 1500 K.

Pd was deposited onto a clean Cu{001} surface from a molten Pd source dropping on a W wire heated to 1200 K. A deposition rate of approximated 1 monolayer/35 min was estimated by comparing with our earlier work.¹ The pressure during deposition was in the high 10^{-10} -Torr range. The LEED pattern was observed to change continuously from the (1×1) characteristic of Cu{001} surface to the best $c(2 \times 2)$ at a Pd coverage of about 0.4 monolayer. The $c(2 \times 2)$ LEED pattern started fading when the Pd coverage became higher than 0.75.

The adsorption of CO on Cu{001} $c(2 \times 2)$ -Pd with various coverages of Pd was first investigated by HREELS at room temperature. CO did not molecularly adsorb on the Cu{001} $c(2 \times 2)$ -Pd surface with a coverage of Pd less than 0.4 monolayer. This is confirmed by the fact that no vibrational loss peak has been observed in the energy range between 200 and 280 meV. This result resembles closely that obtained by Graham using UPS.³ When the coverage of Pd was 0.75 monolayer, however, CO chemisorption was found on the Cu{001} $c(2 \times 2)$ -Pd surface at room temperature. The adsorption was characterized by a vibrational loss at 234 meV which is very close to the bond-stretching frequencies of C-O for bridge bonding on Pd{001} (Ref. 5) and Pd{111}.⁶ This

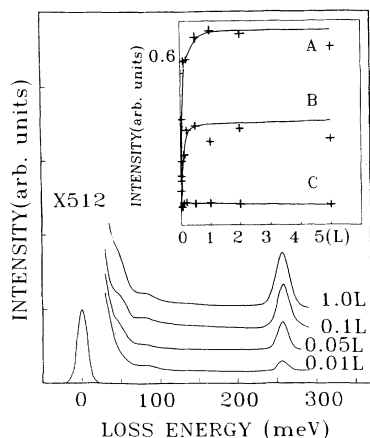


FIG. 1. HREELS for CO/Cu{001} $c(2 \times 2)$ -Pd at 240 K and different CO exposures. Inset shows the normalized intensities of vibrational peaks A (257 meV), B (49 meV), and C (80 meV) dependence on the CO exposures.

suggested that the disordered Pd cluster is also formed on Cu{001} at a Pd coverage lower than this. The vibrational loss at 234 meV is due to the CO adsorbed on the Pd cluster at room temperature. In order to avoid the interference of the Pd cluster, the following spectra which have been taken at low temperature are obtained from the Cu{001} $c(2 \times 2)$ -Pd surface with a Pd coverage less than 0.4 monolayer.

Al was deposited on a clean Ni{001} surface from a molten Al source dropping on a W wire heated to 1600 K and producing an evaporation rate of about 1 monolayer/10 min. The pressure during deposition was in the high 10^{-10} -Torr range. After deposition of 1–2 monolayer of Al, the Ni substrate was annealed at 500°C for 5 min. The LEED pattern changed into a $c(2 \times 2)$ reconstruction. The LEED spectra are similar to those reported in our earlier work.²

III. RESULTS AND DISCUSSION

A. CO on Cu{001} $c(2 \times 2)$ -Pd

Keeping the sample temperature at 240 K, a series of HREELS spectra was taken with various CO exposures (Fig. 1). At this temperature, no vibrational-loss peak, which would be located at 42 and 260 meV, has been observed after 5 L (1 L = 10^{-6} Torr) CO exposure to a clean Cu{001} surface without Pd. It means that this temperature is well above the adsorption temperature of CO on the clean Cu{001} surface as confirmed by Graham.³ Figure 2 shows the HREELS spectra of CO adsorbed on Cu{001} at 135 K. The loss peak at 42 meV is attributed to the Cu-C stretching vibration and the loss peak at 260 meV is attributed to the C-O stretching vibration. The loss peaks of CO on Cu{001} $c(2 \times 2)$ -Pd are at 49, 80, and 257 meV. According to Nguyen and Sheppard,⁷ for CO adsorbed on metal, the CO stretching vibration is in the $2000\text{--}2130\text{-cm}^{-1}$ (248–264-meV) region for on-top CO, in the $1880\text{--}2000\text{-cm}^{-1}$ (233–248-meV) region for twofold-bridged CO, in the $1800\text{--}1880\text{-cm}^{-1}$ (223–233-meV) region for threefold-bridged CO, in $<1800\text{-cm}^{-1}$ (<223 meV) for fourfold-bridged CO. Be-

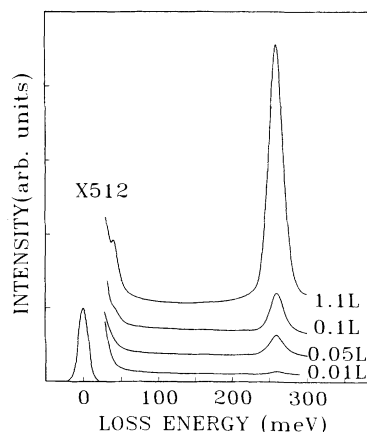


FIG. 2. HREELS for CO/Cu{001} at 135 K.

cause no CO molecules are adsorbed on Cu{001} at 240 K, the loss peak at 257 meV (Fig. 1) is attributed to the C-O stretching vibration for CO species bonded in an on-top position of first-layer Pd atoms, and the loss peak at 49 meV to the C-metal vibration. In contrast to the observation from Pd{001} (Ref. 5) and Pd{111},⁶ no energy-loss peak has been found in the energy range between 210 and 240 meV. This means that no CO molecules were adsorbed at the bridge-bonded position between two Pd atoms. This is consistent with the surface-structure studies by LEED (Ref. 1) of the Cu{001}c(2×2)-Pd-ordered alloy surface where all the nearest neighbors of the Pd atoms in the first layer are Cu atoms.

The inset of Fig. 1 shows that the relative intensities of the vibrational losses at 49 and 257 meV are about 0.5, which is similar to the value on Pd{001},⁵ but much different from the value 0.16 on Cu{001} (Fig. 2). It supports the interpretation that most of the CO molecules are adsorbed on top of Pd atoms but not on top of Cu atoms. UPS studies^{1,3} have shown that for Cu{001}c(2×2)-Pd, the Pd-derived feature is located at 1.7 eV below the Fermi level and well above the Cu 3*d* band. Therefore the CO molecules should more easily interact with Pd atoms than Cu atoms.

Figure 3 depicts the vibrational spectra of CO on Cu{001}c(2×2)-Pd at 135 K. For 0.01-L CO exposure, the spectrum displays two peaks at 51 and 257 meV. Increasing the exposure of CO, the vibration peak at 257 meV is shifted upward to 261 meV and the peak at 51 meV is shifted downward to 44 meV with 2.0-L exposure of CO. The relative intensities of the C-metal vibration (44–51 meV) and the C-O stretching vibration (257–261 meV) depend on the CO exposure in the inset of Fig. 3. For lower CO exposures (<0.1 L), the loss peaks are 51 and 257 meV, they are similar to the features at 49 and 257 meV at 240 K (Fig. 1), and so CO molecules are adsorbed in on-top positions of Pd atoms also. For higher CO exposures (>0.1 L), the loss peaks are shifted to the

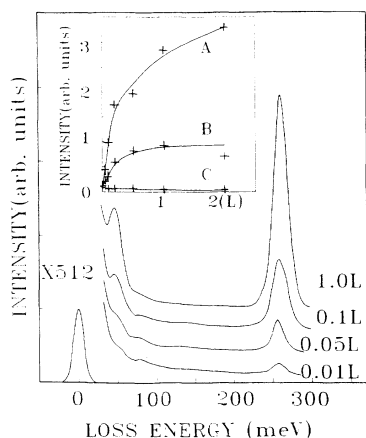


FIG. 3. HREELS for CO/Cu{001}c(2×2)-Pd at 135 K and different CO exposures. Inset shows the normalized intensities of vibrational peaks A (257–261 meV), B (51–44 meV), and C (80 meV) dependence on the CO exposures.

loss peaks of Cu{001} (Fig. 2), and the relative intensities of the C-metal vibration (44–51 meV) and the C-O stretching (257–261 meV) (inset of Fig. 3) tend to saturate, so we claim that the CO molecules are adsorbed in on-top positions of both Pd and Cu atoms of the Cu{001}c(2×2)-Pd surface.

We should note that there is another weak feature which is located at 80 meV in the spectra of Figs. 1 and 3. During CO exposure at 240 K, the 80-meV peak appears first in the HREEL spectra and saturates after 0.1-L exposure. At 135 K, the 80-meV peak has been saturated by the residual gas CO in our system and becomes weaker at high CO exposure. This feature was only observed on the Cu{001}c(2×2)-Pd surface but not on the Cu{001} surface. The feature is attributed to CO because, at room temperature, the intensity of the 80-meV peak increases as the CO exposure increases. During CO adsorption, as the sample temperature increases, the intensity of the 80-meV peak first increases until the two 51- and 257-meV loss peaks disappear in the HREELS spectrum, then decreases and finally disappears at high temperature. If first adsorbing O₂ then adsorbing CO, HREELS spectra show two loss peaks at 46 and 258 meV, but no peak at 80 meV. Because the 80-meV peak is very weak and does not appear after adsorbing O₂, we claim that the Cu{001}c(2×2)-Pd surface has a small number of defects, with CO having been dissociated in defect centers. Some O-metal loss peaks are seen around 80 meV. For example, an Al-O vibrational peak at 68–80 meV (Fig. 4) and W-O peak at 78 meV.⁸ The behavior of the intensity of the 80-meV peak versus CO exposure is quite similar to the 78-meV peak on W{001}. The 80-meV peak is attributed to the O-metal vibration after dissociating CO in defect centers. This peak is only observed after depositing Pd, perhaps with some disordered Pd atoms forming the defect centers.

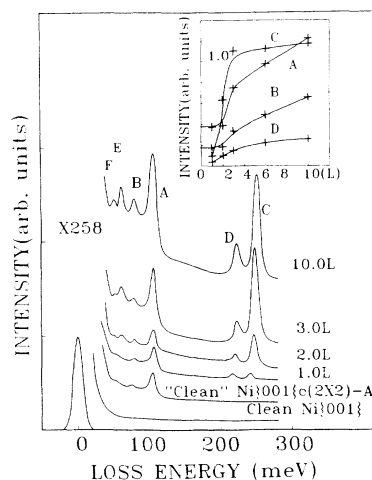


FIG. 4. HREELS for CO/Ni{001}c(2×2)-Al with O of 2 at % at room temperature. Inset shows the normalized intensities of vibrational loss peaks A (105 meV), B (78 meV), C (241–250 meV), and D (217–222 meV) dependence on the CO exposures.

B. CO on Ni{001}c(2×2)-Al

Figure 5(a) is the Auger spectrum of clean Ni{001}, the LEED pattern shows a sharp (1×1) pattern. The LEED pattern and HREELS spectra of CO adsorbed on a clean Ni{001} surface are similar to those of Tracy⁹ and Andersson¹⁰ at room or lower temperatures.

Figure 5(b) is the Auger spectrum of Ni{001}c(2×2)-Al; the LEED pattern shows sharp spots and low background. Figure 5(b) shows that the surface was contaminated by oxygen during Al deposition. The concentration of O is estimated to be about 2 at. %. Figure 4 depicts the HREELS data after various exposures of CO on Ni{001}c(2×2)-Al at room temperature. For the spectrum of "clean" Ni{001}c(2×2)-Al, three vibrational losses at 52, 75, and 105 meV are found. In our experiments their intensities are proportional to the oxygen contamination (Fig. 6). In an earlier work, Erskine and Strong¹¹ have shown that oxygen is adsorbed in both surface and subsurface sites on Al{001}. The vibrational losses at 103–110 and 68–80 meV involve subsurface and surface-oxygen motions, respectively. These vibrational losses were also found by Franchy⁴ in the spectra of oxygen on NiAl{111} after annealing at 800°C. They claim that the 52-meV energy-loss peak is characteristic of the formation of Al₂O₃.

The vibration spectrum of 1.0-L exposure of CO on Ni{001}c(2×2)-Al displays two C-O stretching vibrations at 217 and 241 meV. Increasing the exposure of CO leads to a shift of the two C-O stretching vibrations to

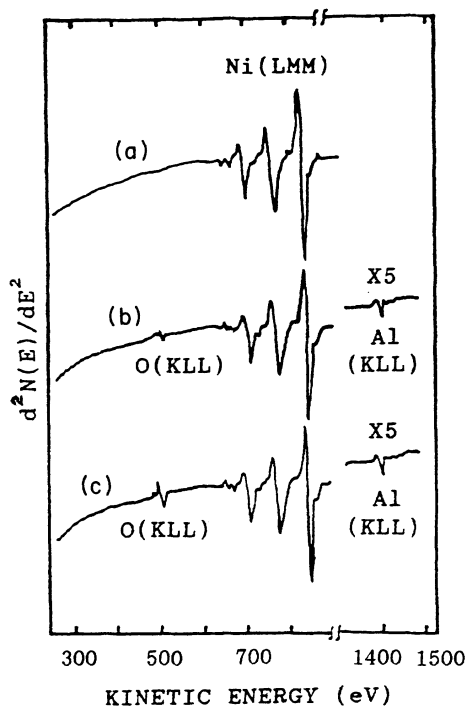


FIG. 5. Auger spectra of (a) clean Ni{001}, (b) Ni{001}c(2×2)-Al with O of 2 at. %, and (c) Ni{001}c(2×2)-Al with O of 6 at. %.

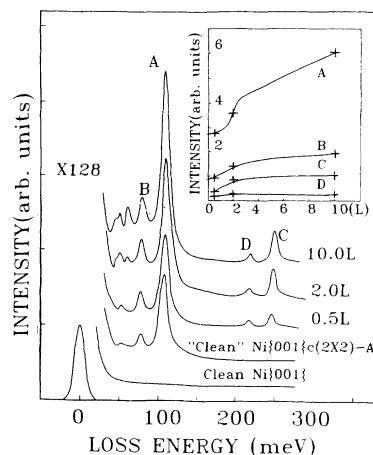


FIG. 6. HREELS for CO/Ni{001}c(2×2)-Al with O of 6 at. % at room temperature. Inset shows the normalized intensities of vibrational loss peaks A (108 meV), B (78 meV), C (246–251 meV), and D (217–222 meV) dependence on the CO exposures.

higher energy, and at saturation coverage (about 10 L) the stretching vibrations of 222 and 250 meV are observed. An increase of CO coverage will decrease the degree of *d*-electron back donation from the Ni atoms into the 2π* antibonding orbital of CO and thus increase the C-O bonding. The C-O bond-stretching vibration at 241–250 meV is characteristic of CO molecules bonded in on-top positions of first-layer Ni atoms as on Ni{001} (Ref. 10) and NiAl{111}.⁴ A striking feature was the observation of the vibrational loss at 217–222 meV instead of the vibrational loss at 239.5 meV on Ni{001} (Ref. 10) and at 235.5 meV on NiAl{111}.⁴ In the latter cases, the CO was bonded in the bridge position between two Ni atoms and one Ni and one Al atom, respectively. According to Nguyen and Sheppard,⁷ the vibrational loss at 217–222 meV is attributed to the C-O bond-stretching vibration of CO molecules bonded in fourfold bridge positions of two Al and two Ni atoms.

The most interesting result was how the intensity of vibrational energy-loss peaks A (105 meV), B (78 meV), C (241–250 meV), and D (217–222 meV) depend on the CO exposures. The dependence of the intensity of peak A on the CO exposures clearly shows that when CO exposure is higher than 2.0 L, CO partial dissociation occurs on the surface. The dissociated oxygen atoms recombine with Al atoms and form some Al oxides on the surface, thus increasing the intensity of peak A. In the inset of Fig. 4, the normalized intensity of peak A increases much faster than that of the peak B as the CO exposure increases. It means that the dissociated oxygen atoms prefer occupying the subsurface sites to the surface sites. This result is consistent with the idea that the surface oxygen phase is unstable and converts to subsurface oxygen at room temperature for Al{001} as claimed by Erskine and Strong.¹¹

The relative intensity of the fourfold bridge position (peak D) to the on-top position (peak C) of CO on Ni{001}c(2×2)-Al is quite small at room temperature.

It suggests that the CO dissociation occurs mostly on the bridge-bonded position. In Fig. 4 HREEL spectra show that most oxygen atoms occupy the subsurface positions. The oxygen contamination will lift the Al atoms above the first atomic layer. This Al atom can act as an efficient dissociation site if the nearest bridge positions are occupied by CO. Then the Al atom reacts with the oxygen atom of CO and forms Al oxide on the surface. This dissociative mode is similar to the CO dissociation on Al{111}.¹² But on the Ni{001} $c(2\times 2)$ -Al surface, the Ni atom acts as an efficient adsorber of CO, thus the dissociation of CO is much easier in our experiment. This dissociation mode is also confirmed by the dissociate-rate dependence on the oxygen contamination. Our experiments show that the CO-dissociation rate is proportional to the degree of oxygen contamination on the surface (Fig. 6).

There are some small changes in the loss-energy range between 40 and 70 meV in Fig. 4. When the CO exposure reaches 2.0 L, a feature *E* appears at 60 meV, which is due to the Ni-CO bond-stretching vibration.¹⁰ After CO exposure is higher than 3.0 L, another peak, *F*, shows up at the lower loss-energy side of the 60-meV peak, somewhere around 50 meV. We suggest that this is due to the dissociated C atom adsorbed on the surface.

The normalized intensity of peak *A* stays constant below 2.0-L CO exposure and then shows a remarkable increase as the CO exposure exceeds 3.0 L. This result precludes the possibility that the intensity increase of peak *A* is caused by the residual oxygen.

More oxygen contamination will provide more efficient dissociation sites for CO. Figure 5(c) shows that the relative intensity of O is about three times that of Fig. 5(b). This means the concentration of O is about 6 at. %. Figure 6 is the HREEL spectra of CO adsorbed on this surface at room temperature. For the spectrum of "clean" Ni{001} $c(2\times 2)$ -Al, there are three vibrational losses at 52, 78 (*B*), and 108 (*A*) meV in Fig. 6. They correspond to Al₂O₃, surface, and subsurface oxygen motions, respectively. Peak *A* of Fig. 6 is higher than peak *A* of Fig. 4. This also explains why the intensity of the 108-meV peak is reflected in the amount of oxygen on the surface. The vibrational spectrum of 0.5-L exposure of CO displays two vibrational peaks at 217 and 246 meV. They involve the C-O bond-stretching vibrations on fourfold bridge positions of Al and Ni atoms and the on-top position of Ni atoms. Increasing the exposure of CO leads to a shift of the two peaks to 222 and 251 meV at saturation coverage (about 10 L). Increasing the CO coverage leads to an increase of the intensity of the 246-meV vibrational peak, but no change in the intensity of the 217-meV vibrational peak. In the inset of Fig. 6, the normalized intensity of the 108-meV peak (*A*) increases much faster than the same peak in Fig. 4 with increasing CO exposures. This suggests that the CO-dissociation rate is proportional to the degree of oxygen contamination on the surface. In Fig. 6 more Al atoms were lifted from the first atomic layer by the subsurface oxygen atoms, thus providing more efficient dissociation sites for CO. The constant intensity of the 217-meV peak with increasing CO exposure is also explained by the CO dissociation occurring on the

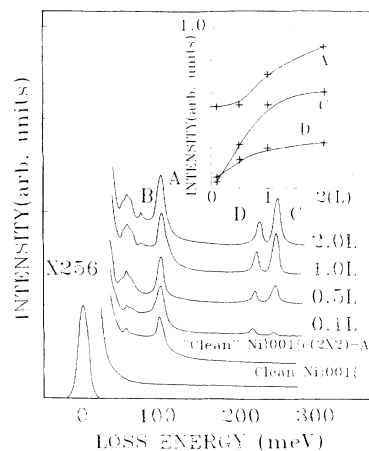


FIG. 7. HREELS for CO/Ni{001} $c(2\times 2)$ -Al with O of 2 at. % at 135 K. Inset shows the normalized intensities of vibrational loss peaks *A* (100 meV), *C* (247–250 meV), and *D* (217–226 meV) dependence on the CO exposures.

fourfold bridge position.

Figure 7 depicts the HREELS data after various CO exposures on Ni{001} $c(2\times 2)$ -Al at low temperature (135 K). Before CO adsorption, the spectrum displays two vibrational losses at 55 and 100 meV, which correspond to the vibrations of Al₂O₃ and subsurface oxygen atoms. This also means that no oxygen atoms lie on the surface. The spectrum of 0.1-L CO displays two C-O bond-stretching vibration peaks at 217 and 247 meV and a small peak at the high-energy side of 55 meV (metal-CO vibration). The intensities of three peaks increase with increasing CO exposure and the 217- and 247-meV peaks shift to 226 and 250 meV at saturation coverage (2.0 L). The spectrum of 0.5 L displays a small peak on the low-energy side of 55 meV. It corresponds to the C-metal vibration after CO dissociation. When the CO exposure is increased to 1.0 L, a loss peak at 75 meV is found. It corresponds to the vibration between surface oxygen and metal. Surface oxygen atoms are from the dissociated CO. At low temperature, the adsorption coefficient of CO is increased; thus CO dissociation is observed at low exposure (0.1 L), but the CO-dissociation rate at 135 K is weaker than at room temperature.

IV. CONCLUSION

Finally, we summarize the different adsorption behaviors of CO between Cu{001} $c(2\times 2)$ -Pd and Ni{001} $c(2\times 2)$ -Al surfaces. On a Cu{001} $c(2\times 2)$ -Pd surface, CO molecules are bonded only in on-top positions of Pd atoms at 240 K and the energy position of the CO stretching vibrational loss peak, which is located at 260 meV, is independent of the CO coverage. For Ni{001} $c(2\times 2)$ -Al, CO molecules are bonded in on-top positions of Ni atoms and also "fourfold" bridge positions between two Al and two Ni atoms. Increasing the CO exposure leads to a shift of the two C-O bond-stretching vibrations from 217 and 241 meV to 222 and 250 meV, respectively. These differences could be ex-

plained by their different atomic structures. The $\text{Cu}\{001\}c(2\times 2)$ -Pd phase consists of a mixed layer of alternating Pd and Cu atoms on the top layer of the $\text{Cu}\{001\}$ substrate with no Pd atoms in the second layer, but in the $\text{Ni}\{001\}c(2\times 2)$ -Al phase, the first layer is a mixed-layer of alternating Ni and Al atoms and the second layer is occupied only by Ni atoms. So the "four-fold" bridge positions between two Al and two Ni atoms in the first layer are also the on-top positions of the Ni atoms in the second layer and should be favorable for CO adsorption. We note that the Pd atoms in the $\text{Cu}\{001\}c(2\times 2)$ -Pd phase are more isolated than the Ni atoms in the $\text{Ni}\{001\}c(2\times 2)$ -Al phase. The d electrons, which back-donated into the $2\pi^*$ antibonding orbital of CO, come from the Ni atoms not only in the first layer

but also in the second layer. So the energy positions of C-O bond-stretching vibrational-loss peak are more sensitive to the CO coverage on $\text{Ni}\{001\}c(2\times 2)$ -Al than on $\text{Cu}\{001\}c(2\times 2)$ -Pd.

In summary, we have reported in this work the observation of CO dissociation on Ni-Al alloy surfaces at room and lower temperatures.

ACKNOWLEDGMENTS

The authors are grateful to Qingzhe Zhang, Dr. Changheng Wang, and Chizi Liu for their skillful technical assistance. This work was supported by the National Nature Science Foundation of China, under Grant No. 19074004.

-
- ¹S. H. Lu, Z. Q. Wang, S. C. Wu, C. K. C. Lok, J. Quinn, Y. S. Li, D. Tian, F. Jona, and P. M. Marcus, *Phys. Rev. B* **37**, 4296 (1988); S. C. Wu, S. H. Lu, Z. Q. Wang, C. K. C. Lok, J. Quinn, Y. S. Li, D. Tian, F. Jona, and P. M. Marcus, *ibid.* **38**, 5363 (1988).
²S. H. Lu, D. Tain, Z. Q. Wang, Y. S. Li, F. Jona, and P. M. Marcus, *Solid State Commun.* **67**, 325 (1988).
³G. W. Graham, *Surf. Sci.* **171**, L432 (1986).
⁴R. Franchy, M. Wutting, and H. Ibach, *Surf. Sci.* **189/190**, 438 (1987).
⁵R. J. Behm, K. Christmann, G. Ertl, M. A. Van Hove, P. A.

- Thiel, and W. H. Weinbery, *Surf. Sci.* **88**, L59 (1979).
⁶A. M. Bradshaw and F. M. Hoffmann, *Surf. Sci.* **72**, 513 (1979).
⁷T. T. Nguyen and N. Sheppard, in *Advances in Infrared and Raman Spectroscopy*, edited by R. E. Hester and R. H. J. Clark (Heyden, London, 1978), Vol. 5.
⁸R. Franchy and H. Ibach, *Surf. Sci.* **155**, 15 (1985).
⁹J. C. Tracy, *J. Chem. Phys.* **59**, 2736 (1972).
¹⁰S. Andersson, *Solid State Commun.* **21**, 75 (1977).
¹¹J. L. Erskine and R. L. Strong, *Phys. Rev. B* **25**, 5547 (1982).
¹²K. Khonde, J. Daroill, and J. M. Gills, *Surf. Sci.* **126**, 414 (1983).